

# On the Mechanism of the Volume Reflection of Relativistic Particles \*

G. V. Kovalev

North Saint Paul, MN 55109, USA

(Dated: Feb. 15, 2008)

The mechanisms of the volume reflection of positively and negatively charged relativistic particles in a bent crystal have been analyzed. It has been shown that the empty core effect is significant for the negatively charged particles. The average reflection angle of the negatively charged particles has been determined and the conditions for the observation of the reflection and refraction are discussed.

PACS numbers: 13.88.+e, 41.60.-m, 61.85.+p

The experiments reported in [1-3] confirmed the effect of the volume reflection of 1-, 70-, and 400-GeV protons in a bent Si crystal, which was revealed by Taratin and Vorobiev [4, 5] using the Monte Carlo method, and demonstrated the possibility of its application to collimate accelerated beams [6]. The numerical calculations performed in [4, 5, 7] also indicated the volume reflection of negatively charged particles, but the corresponding reflection angle is smaller than that for positively charged particles. However, the reflection of the negatively charged particles differs in nature from the reflection of the positively charged particles and requires a more detailed analysis. Indeed, within the framework of classical mechanics, the reflection and scattering of the negatively charged particles in the field of a one-dimensional potential well (see Fig. 1a) are absent, whereas the grazing incidence of the positively charged particles on a one-dimensional barrier,  $\alpha < \theta_L$  ( $\alpha$  is the angle between the particle momentum and the boundary of the one-dimensional barrier and  $\theta_L$  is the Lindhard critical angle, see Fig. 1b), is accompanied by the complete reflection. For the case of a centrally symmetric potential, this phenomenon is responsible for the volume reflection of positively charged relativistic particles in a bent crystal. Indeed, the impact parameter  $b$  measured from the tangential edge (point  $T$  in Fig. 1c) of the centrally symmetric ring barrier with the height  $U_o$  is given by the expression  $b = R(1 - \cos(\alpha))$  and the average reflection angle is specified by the integral

$$\bar{\chi} = \frac{1}{b_{max}} \int_0^{b_{max}} 2\alpha db, \quad (1)$$

Here, the maximum impact parameter,  $b_{max} = R(1 - \cos(\theta_L))$ , depends on the critical channeling angle  $\theta_L = \sqrt{2U_o E/(p^2 c^2)}$  and the potential-barrier radius  $R$ . For small angles  $\alpha$ ,  $\theta_L \ll 1$ ,  $b_{max} = R\theta_L^2/2$ ,  $db = R\alpha d\alpha$ , and Eq. (1) provides the average reflection angle

$$\bar{\chi} = 4\theta_L/3, \quad (2)$$

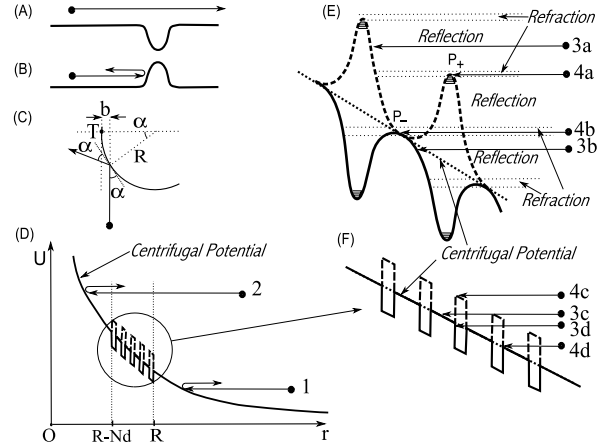


FIG. 1: One-dimensional motion of the (a) negatively and (b) positively charged particles, (c) the reflection of a positively charged particle from the centrally symmetric barrier, (d) the effective potential of the system of rectangular ring potentials, (e) the reflection and refraction regions, and (f) the liner approximation for the effective potential.

coinciding with the estimate obtained for the bent crystal Eq. (18) in [8].

On the contrary, it is well known that the reflection is absent in the case of scattering on the centrally symmetric potential well with the depth  $-U_o$ . In this case, only refraction occurs for all impact parameter values (see problem 2 in Sect. 19 in [9]). Thus, the reflection of the negatively charged particles in the numerical simulation is at first sight surprising. Nevertheless, as shown in [8], the negatively charged particles scattered on a ring potential undergo reflection. Since the presence of the inner potential wall distinguishes the ring potential from the potential well, it is natural to think that this reflection is the reflection from the inner potential wall of the ring potential similar to the reflection from the outer wall of the potential barrier. However, as shown below, the determining factor of the reflection of the negatively charged particles in a crystal is the effect of a specific deflection called the empty core effect [8].

For the scattering in a central field (and in a uniformly bent crystal), the following effective potential is intro-

\*JETP Letters, 2008, Vol. 87, No. 7, pp. 349-353

duced:

$$U_{eff}(r) = U(r) + \frac{p_\infty^2 c^2 b^2}{2Er^2}, \quad (3)$$

where  $b$  is the impact parameter measured from the center and the remaining symbols are the same as in [8]. In this potential, any infinite motion formally looks like a reflection; i.e., a particle comes from infinity, stops at the turning point, and goes away to infinity.

We emphasize that such treatment of the reflection is not necessarily valid [3]. The first example is trivial: particle 1 in Fig. 1d is reflected at the distance  $b > R$  from the center of the effective potential, which includes only the centrifugal term, because  $U(r) = 0$  in this region. This motion in the Cartesian coordinates is a rectilinear motion. For the second example, particle 2 in Fig. 1d is reflected at the distance  $b < RNd$  from the center of the ring potential, where also  $U(r) = 0$ . This is the empty core effect. As shown in [8], two opposite situations are possible. First, a particle with any trajectory similar to trajectory 2 in Fig. 1d is reflected (has the angle  $\chi > 0$ ) in an arbitrary negative nonsingular potential localized in a ring. Second, a particle whose trajectory is similar to trajectory 2 in Fig. 1d is refracted (has the angle  $\chi < 0$ ) in a positive nonsingular ring potential. In both cases, the turning point is the same and lies on the centrifugal curve. Finally, let us consider the examples where the turning point lies in the crystal potential  $U(r)$ . They are in close connection with the experiments on the reflection of relativistic particles. Figures 1d and 1f show the effective potential of the system of periodic rings used in [8]. The real crystal potential is a smooth function and, if the Tsyganov criterion  $R > \frac{p_\infty^2 c^2}{U(r)}$  [10] is satisfied, the effective potential has the system of smooth maxima and minima corresponding to each bent potential plane (see Fig. 1e).

In the 1950s, Ford and Wheeler [11, 12] showed that, if the effective potential for a certain impact parameter has a smooth local maximum, the deflection function [13]

$$\chi(b) = \pi - 2\sqrt{\frac{p_\infty^2 c^2 b^2}{2E}} \int_{r_0}^{\infty} \frac{\frac{1}{r^2} dr}{\sqrt{\frac{p_\infty^2 c^2}{2E} - U(r) - \frac{p_\infty^2 c^2 b^2}{2Er^2}}}, \quad (4)$$

has a negative logarithmic singularity; i.e., the particle incident on the maximum of the potential undergoes an indefinite number of rotations about the center. This phenomenon of spiral or orbital scattering was well known in low-energy atomic collisions [14, 13]. Under certain conditions, this mechanism also occurs for relativistic particles. If the particle trajectories touch the effective potential at the local-maximum points (trajectories 4a and 4b in Fig. 1e), not only the radial velocity of the particle,  $v_r$ , but also the radial force  $-\partial U_{eff}/\partial r$  (and, therefore, the radial acceleration  $\dot{v}_r$ ), vanish at these points. This means that the particle motion in the

radial direction ceases, whereas the particle continues to move in the tangential direction (the circle with the radius  $r_0$  is a limit cycle which the particle approaches along a spiral). This is the classical spiral-scattering mechanism. If losses were absent, the particle could execute an infinite number of rotations about the center. This position is evidently unstable and small fluctuations move the particle out of this state. Resonant scattering is a quantum-mechanical analog of this phenomenon [15]. Strictly speaking, only one trajectory satisfies the spiral scattering conditions. For trajectories close to this trajectory, this effect in classical mechanics is manifested as the refraction: the particle, passing a small part of the angular path towards the potential bend, is deflected and moves away from the center along the symmetric asymptotic curve. The reflection and refraction regions are shown in Fig. 1e by the dashed lines.

However, in the experiments on the reflection of positively charged particles [1-3], the volume capture of protons into the channeling regime was observed instead of the spiral scattering. In my opinion, this is due to two important causes. First, the crystal nucleus density and electron density (dark regions in Fig. 1e) are high at maxima for positively charged particles. Second, the spiral scattering and refraction of the positively charged particles ensure a quite long-term presence of particles near the maxima of the effective potential and, therefore, strongly increase the intensity of the volume capture. The maximum of the potential for negatively charged particles is a wider concave parabola; hence, the refraction region for the negatively charged particles should be wider. The crystal nucleus density and electron density almost vanish at the maxima for the negatively charged particles. Therefore, the stability of the refraction trajectories for the negatively charged particles in a narrow impact-parameter range should be much higher. As a result, a fraction of the negatively charged particles in the narrow impact-parameter range can move towards the crystal bend without the mechanism of volume capture into the channeling regime due to the refraction near the local maxima of the potential and a related mechanism, that is, the spiral scattering. In this case, the peak characteristic of the volume capture of the positively charged particles should be absent for the capture of the negatively charged particles. Thus, the effect of the refraction and spiral scattering can be noticeable in a detailed comparison of the scatterings of positively and negatively charged relativistic particles in the region traditionally treated as the volume capture region. The exact solution of the problem of scattering on the potential of the periodic system of rectangular rings was considered in [8], where the average angle of the reflection of positively charged relativistic particles that describes the experiments reported in [1-3] was also estimated. In the model of the rectangular rings, the potential is not a smooth function and the radial force does not vanish at the tan-

gent points (see, e.g., lines 4c and 4d in Fig. 1f); hence, the spiral scattering is absent in this model. However, it is applicable for describing the reflection (see lines 3c and 3d in Fig. 1f) including the reflection of negatively charged relativistic particles; the details of this description are given below. First, most trajectories of negatively charged particles have the turning points lying on the centrifugal potential curve between potential wells (see curve 3c in Fig. 1f) and a few trajectories enter the potential well regions (see curve 3d in Fig. 1f). Since the crystal potential lying above the trajectory (line 3c) does not affect the behavior of the particle, it is easy to see that the scattering of the particle with a trajectory similar to line 3c has the same nature as the scattering of the particle with trajectory 2 in Fig. 1d; i.e., the turning angle, in this case, is determined by the empty core effect. Since the potential lying under the particle trajectory is negative, the reflection occurs for trajectories of type 3c. This qualitatively explains Figs. 2c and 2d in [8] and Fig. 2a in this paper, where the angles in the region on the left of the point 1 are positive. Formula (15) in [8] contains a misprint. The correct expression for the scattering of negatively charged particles on one ring that was used to plot Figs. 2c and 2d in [8] has the form

$$\alpha(\hat{b})_- = \quad (5)$$

$$\begin{cases} (\sqrt{1-\hat{b}^2} - \sqrt{\Phi-\hat{b}^2}) - (\sqrt{1-\hat{b}_a^2} - \sqrt{\Phi-\hat{b}_a^2}), \\ \text{for } 0 < \hat{b} < (1-\hat{a}); \\ \sqrt{1-\hat{b}^2} - \sqrt{\Phi-\hat{b}^2} + \sqrt{\Phi-\hat{b}_a^2}, \\ \text{for } (1-\hat{a}) < \hat{b} < (1-\hat{a})\sqrt{\Phi}; \\ \sqrt{1-\hat{b}^2} - \sqrt{\Phi-\hat{b}^2}, \text{ for } (1-\hat{a})\sqrt{\Phi} < \hat{b} < 1; \\ 0, \text{ for } 1 < \hat{b}. \end{cases}$$

Some of Eqs. (16) in [8] for the maximum and minimum deflection angles of negatively charged particles should be written as

$$\begin{aligned} \alpha_{max-} &= \sqrt{2\hat{a}} - \sqrt{2\hat{a} - \phi_o} - \sqrt{-\phi_o} \\ \alpha_{min-} &= -\sqrt{-\phi_o}. \end{aligned} \quad (6)$$

They are obtained from Eq. (5) using the substitutions  $\hat{b} = (1-\hat{a})$  and  $\hat{b} = 1$  and the smallness conditions  $\hat{a} \ll 1$  and  $\hat{a}^2 \ll \hat{a}$ . When the well is sufficiently deep,  $|\phi_o| > 2\hat{a}$ , these formulas are modified to the form

$$\begin{aligned} \alpha_{max-} &= \sqrt{2\hat{a}} - \frac{\hat{a}}{\sqrt{|\phi_o|}} \\ \alpha_{min-} &= -\frac{\hat{a}}{\sqrt{|\phi_o|}}. \end{aligned} \quad (7)$$

In this case, the range  $(1-\hat{a})\sqrt{\Phi} < \hat{b} < 1$  contracts to zero. This is seen in Figs. 2d and 3d in [8] (cf. Figs.

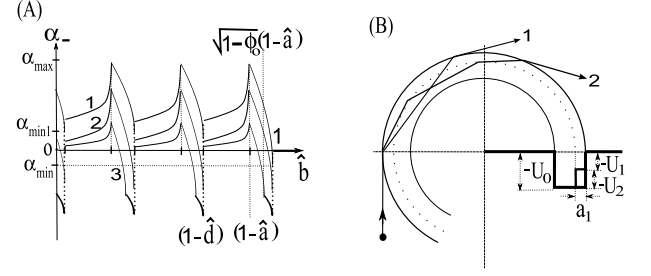


FIG. 2: (a) Deviation functions for negatively charged particles at  $\phi_o/\hat{a}$ : 1 -  $\phi_o/\hat{a} = 12$ , 2 -  $\phi_o/\hat{a} = 4$ , 3 -  $\phi_o/\hat{a} = 1.2$ ; (b) The tangential scattering trajectory on (1) the square potential well and (2) step potential with the same maximum depth as for the square potential well  $U_0 = U_1 + U_2$ .

2c and 3c in [8]), where the lower part of the deflection function corresponding to the bottom of the potential well disappears.

The general expression for the deflection function of negatively charged particles in the system of rectangular rings [8], when the impact parameter lies in the ring  $(k+1)\hat{d} < \hat{b} < (1-k\hat{d})$ , has the form

$$\chi(\hat{b})_- = 2 \sum_{i=0}^{k-1} \alpha_i(\hat{b}) + \quad (8)$$

$$+ 2 \begin{cases} (\sqrt{1-\hat{b}_k^2} - \sqrt{\Phi-\hat{b}_k^2}) - (\sqrt{1-\hat{b}_{ka}^2} - \sqrt{\Phi-\hat{b}_{ka}^2}), \\ \text{for } (1-(k+1)\hat{d}) < \hat{b} < (1-\hat{a}-k\hat{d}); \\ \sqrt{1-\hat{b}_k^2} - \sqrt{\Phi-\hat{b}_k^2} + \sqrt{\Phi-\hat{b}_{ka}^2}, \\ \text{for } (1-\hat{a}-k\hat{d}) < \hat{b} < (1-\hat{a}-k\hat{d})\sqrt{\Phi}; \\ \sqrt{1-\hat{b}_k^2} - \sqrt{\Phi-\hat{b}_k^2}, \\ \text{for } (1-\hat{a}-k\hat{d})\sqrt{\Phi} < \hat{b} < (1-k\hat{d}). \end{cases}$$

The deflection function calculated using Eq. (8) with various values of the parameter  $2U_oE/(p_\infty^2 c^2 \hat{a})$  is shown in Fig. 2a as a function of the potential depth  $U_o$ .

The average reflection angle for negatively charged particles can be calculated from the potential period nearest to the edge. When the reflection from the inner potential wall is disregarded, this angle is determined by the integral

$$\bar{\alpha}_- = \frac{1}{\hat{d}-\hat{a}} \int_{1-\hat{d}}^{1-\hat{a}} \left( (\sqrt{1-\hat{b}^2} - \sqrt{\Phi-\hat{b}^2}) - (\sqrt{1-\hat{b}_a^2} - \sqrt{\Phi-\hat{b}_a^2}) \right) d\hat{b} \quad (9)$$

with subsequent expansion in small quantities  $\hat{a}, \hat{d}$  and  $\phi_o$ . As a result, the expression for the average reflection angle  $\bar{\chi}_- = 2 \cdot \bar{\alpha}_-$  for negatively charged particles is obtained in the form

$$\bar{\chi}_- = \frac{2}{3(\hat{d}-\hat{a})} \left( (2\hat{d}-2\hat{a}-\phi_o)^{3/2} + (2\hat{d})^{3/2} + \right.$$

$$(2\hat{a} - \phi_o)^{3/2} - (-\phi_o)^{3/2} - (2\hat{d} - \phi_o)^{3/2} - (2\hat{a})^{3/2} - (2\hat{d} - 2\hat{a})^{3/2}). \quad (10)$$

Formula (10) applied to possible experiments on the scattering of 1-, 70-, and 400-GeV antiprotons with the same geometry of crystals as in [1-3] yields the average reflection angles 14.8, 4.3, and 1.8 mrad, respectively.

In conclusion, let us discuss the possibility of an improvement in the rectangular-ring model that could include the spiral scattering. The refraction angle of the tangential trajectory for the system of rectangular steps that is close to the actual potential curve is larger than the angle for the rectangular well. This relation is seen from the following example. For the tangential trajectory of the negatively charged particle, the refraction angle [minimum angle in Eqs. (6)] for the square potential well with the depth  $U_0$  is  $\alpha_{min-} = -\sqrt{-\phi_o}$ , where  $\phi_o = -\frac{2U_o E}{p_\infty^2 c^2}$ .

Let us consider a step potential shown in Fig. 2b with arbitrary  $U_1$  and  $U_2$  values satisfying the condition  $U_0 = U_1 + U_2$ . For the same tangential trajectory, the deflection angle on the step with the depth  $-U_1$  is  $-\sqrt{-\phi_1}$ , where  $\phi_1 = -\frac{2U_1 E}{p_\infty^2 c^2}$ .

If the step width  $a_1$  is chosen so that the trajectory touches the boundary of the step or intersects the boundary (such choice is always possible), the secondary refraction appears at the angle  $-\sqrt{\phi_2}$ , where  $\phi_2 = -\frac{2U_2 E}{p_\infty^2 c^2}$ .

The total refraction angle is  $-(\sqrt{-\phi_1} + \sqrt{-\phi_2})$  with the condition  $\phi_0 = \phi_1 + \phi_2$ . Since the inequality  $\sqrt{A} + \sqrt{B} > \sqrt{A+B}$  is always valid, the total scattering angle on the step potential,  $\sqrt{-\phi_1} + \sqrt{-\phi_2}$ , is larger than the angle  $\sqrt{-\phi_1 - \phi_2} = \sqrt{-\phi_o}$  on the square well potential, although the maximum depths of these potentials are the

same. Subsequently dividing the potential into smaller steps, one can unlimitedly increase the refraction angle, thus realizing the spiral scattering on the step potential of a finite depth.

- 
- [1] Yu. M. Ivanov, A. A. Petrunin, V. V. Skorobogatov, and et al. *Phys. Rev. Lett.*, 97, 144801, (2006).
  - [2] Yu. M. Ivanov, N. F. Bondar, Yu. A. Gavrikov, and et al. *JETP Letters*, 84(7), 372, (2006).
  - [3] W. Scandale, D. A. Still, A. Carnera, and et al. *Phys. Rev. Lett.*, 98, 154801, (2007).
  - [4] A. M. Taratin and S. A. Vorobiev. *Phys. Lett.*, A 119(8), 425, (1987).
  - [5] A. M. Taratin and S. A. Vorobiev. *Nucl. Instrum. Meth. B*, 26, 512, (1987).
  - [6] W. Scandale, A. Carnera, G.D. Mea, and et al. *Phys. Lett. B*, 658, 109, (2008).
  - [7] V.M. Biryukov. arXiv/0611249.
  - [8] G. V. Kovalev, *JETP Letters*, 87(2), 94, (2008).
  - [9] L. D. Landau and E. M. Lifshitz. *Mechanics (Course of Theoretical Physics, Volume 1)*. Butterworth-Heinemann; 3rd edition, NY, (1976).
  - [10] E. N. Tsyganov. *Fermilab, TM-682*, page 5, (1976).
  - [11] K. W. Ford and J. A. Wheeler. *Annals of Physics*, 7, 259, (1959).
  - [12] K. W. Ford and J. A. Wheeler. *Annals of Physics*, 7, 287, (1959).
  - [13] R. Newton. *Scattering Theory of Waves and Particles, 2nd Ed.* Springer-Verlag, New York, (1982).
  - [14] J.O. Hirschfelder, Ch. F. Curtiess, and R. B. Bird. *Molecular theory of gases and liquids, 2nd Ed.* John Wiley and Sons, New York, (1964).
  - [15] M. V. Berry and K.E. Mount. *Rep. Prog. Phys.*, 35, 315, (1972).